Progress Towards Digital Twin Integration for Online Battery Health Estimation in the SWIFT-UAV Platform

Mateo E. Garcia-Sandoval*, Korebami O. Adebajo†, Matthew Burnett‡, Vaishali Allibada§, and Dr. Austin R.J. Downey¶

Effective digital twin integration is increasingly critical for the optimal operation of unmanned aerial vehicles (UAVs) as missions demand greater autonomy, endurance, and reliability. Traditional UAV battery health monitoring and control strategies rely primarily on onboard sensors, static voltage thresholds, conservative safety margins, and post-flight analysis. While these battery monitoring approaches provide baseline protection, they often result in overly conservative mission planning or reactive warnings that occur too late to prevent degradation or failure. Conventional monitoring methods frequently lack predictive capability, limiting their ability to provide actionable insight during dynamic flight conditions.

To address these challenges, this work presents the development and ground-based validation of a propulsion subsystem digital twin integrated within the SWIFT-UAV (Scientific Workhorse for In-Flight Field Tests), a modular 3D printed UAV platform initially developed at the University of South Carolina. SWIFT-UAV's open architecture, high payload capacity, and compatibility with advanced autonomy make it an ideal testbed for digital twin implementation. Rather than immediate in-flight deployment, the digital twin framework is evaluated using a propulsion iron-bird configuration that isolates the electrical power subsystem from aerodynamic and flight control uncertainties.

Experimental measurements are compared against MATLAB/Simulink Simscape-based propulsion and battery models to assess predictive fidelity and identify discrepancies between modeled and observed behavior. Results demonstrate strong agreement between simulated and experimental data, supporting the feasibility of subsystem-level digital twin validation as a precursor to hardware-in-the-loop and eventual in-flight implementation. This work advances UAV energy management by transitioning from passive threshold-based monitoring toward predictive, model-informed battery endurance forecasting capable of supporting adaptive and energy-aware mission planning.

I. Nomenclature

SOC = State of Charge
RUL = Remaining Useful Life
SOH = State of Health
$C - rate$ = Charge/discharge rate relative to battery capacity
DT = Digital Twin
UAV = Unmanned Aerial Vehicles

II. Introduction

UAVs are increasingly being deployed in various mission environments, including recreational, industrial, scientific, and defense environments. This surge has also created a rising demand for extended endurance, greater autonomy, and higher system reliability [1]. As missions rise in complexity, the need for accurate real-time awareness of system health and energy state becomes a limiting factor in operational safety and performance. The electrical subsystem, most commonly the Lithium-ion Polymer (LiPo) batteries, often represents the primary operational constraint [2]. Battery

*Undergraduate Research Assistant, Department of Mechanical Engineering, University of South Carolina, Columbia, SC 29208, USA.
†Graduate Research Assistant, Department of Mechanical Engineering, University of South Carolina, Columbia, SC 29208, USA.
‡Graduate Research Assistant, Department of Mechanical Engineering, University of South Carolina, Columbia, SC 29208, USA.
§Undergraduate Research Assistant, Department of Mechanical Engineering, University of South Carolina, Columbia, SC 29208, USA.
¶Associate Professor, AIAA Member, Department of Mechanical Engineering, Department of Civil, and Environmental Engineering, University of South Carolina, Columbia, SC 29208, USA, Contact Author austindowney@sc.edu

performance degradation, voltage sag under high discharge rates, and aging-induced capacity fade directly influence endurance and can lead to premature mission termination or unexpected failure.

Conventional UAV energy management strategies rely primarily on onboard voltage thresholds, conservative safety margins, and post-flight analysis. While these approaches provide baseline protection, they often result in overly conservative mission planning or reactive warnings that occur too late to prevent system degradation [3]. Moreover, battery dynamics are nonlinear and highly dependent on load profile, C-ratings, and aging state, making accurate endurance prediction under real mission conditions challenging. As UAV autonomy advances, energy management must evolve from static threshold monitoring toward predictive, model-based intelligence. Digital twin technology provides a promising pathway toward this evolution [4]. A digital twin is a dynamic, high-fidelity virtual representation of a physical system that continuously synchronizes with real-world telemetry to estimate hidden states and forecast future behavior [5, 6]. In aerospace applications, digital twins have been explored for structural health monitoring, propulsion diagnostics, and system-level prognostics [7]. When applied to battery systems, digital twin frameworks can integrate physics-based electrochemical models with real-time telemetry to estimate state of charge (SOC), state of health (SOH), and remaining useful life (RUL) while forecasting mission endurance under anticipated load conditions [3]. In this study, SOH is represented using a voltage-based proxy (VSI) and does not represent long-term capacity degradation.

This work presents the ongoing development and ground-based validation of a digital twin framework integrated into the SWIFT-UAV [8], developed by the ARTS Laboratory at the University of South Carolina. Rather than immediate in-flight implementation, the framework is at present evaluated using a propulsion iron-bird test configuration, allowing isolation of the electrical components of the propulsion subsystem. The iron-bird configuration enables controlled throttle sweeps at varying power levels while measuring motor current, voltage response, and power consumption under repeatable conditions. Experimental measurements are compared against a MATLAB/Simulink Simscape-based propulsion and battery model to quantify model fidelity and identify discrepancies between predicted and observed behavior. By isolating the power subsystem from aerodynamic and flight-control uncertainties, this study focuses on the validation of the digital twin's ability to capture electrical current, load-induced voltage sag, and power response characteristics. Instead of relying on fixed operational limits, the digital twin is continuously meant to forecast endurance under current and anticipated load conditions, enabling informed decision-making such as adaptive throttle control, mission rerouting, early return-to-home triggers, and predictive maintenance scheduling [9]. The contributions of this work are twofold. First, a physics-based digital twin of the SWIFT-UAV propulsion subsystem is developed and validated using a controlled iron-bird experimental configuration. Second, the framework demonstrates predictive battery endurance estimation under varying throttle conditions, enabling a transition from static threshold monitoring to model-informed energy management.

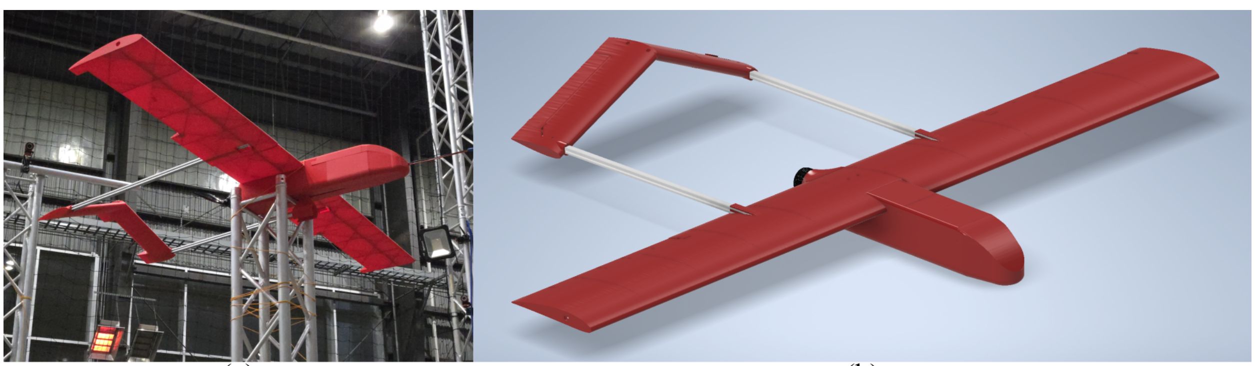

(a) (b)

Fig. 1 SWIFT-UAV (a) physically assembled and (b) CAD assembly model.

III. Methodology

The methodology employed in this study consists of three primary components; The characterization of the propulsion subsystem hardware, the development of a digital twin framework representing the electrical and electromechanical dynamics of the system, and a controlled experimental validation using a ground-based iron-bird configuration. As shown in Fig. 1, (a) illustrates the UAV integrated within the iron-bird test configuration, while (b) presents the corresponding CAD model used during structural and subsystem design. The propulsion subsystem of the SWIFT-UAV was isolated from aerodynamic and flight-control influences in order to focus exclusively on electrical behavior under variable loading conditions. This isolation enables repeatable testing while minimizing uncertainty introduced by lift, drag, and vehicle dynamics. Real-time measurements of voltage and current were collected during controlled throttle sweeps and used both for model input and validation.

The digital twin is designed to synchronize with experimentally measured telemetry and estimate internal states such as power consumption and endurance under varying load conditions. Model predictions are compared directly against experimental measurements to quantify predictive fidelity. This structured approach allows subsystem-level validation prior to hardware-in-the-loop and eventual in-flight integration. The following subsections describe the physical propulsion system, the digital twin modeling framework, and the experimental configuration used for validation. The setup of the electronic subsystem of the UAV and experimental setup is shown in Figure 2.

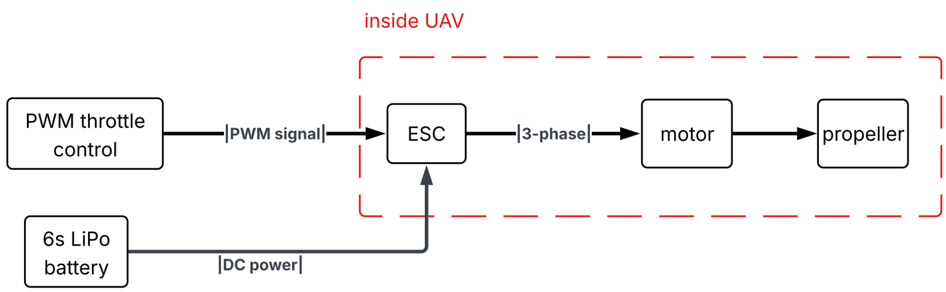

Fig. 2 SWIFT-UAV propulsion subsystem block diagram.

A. Digital Twin

The digital twin framework is implemented in MATLAB/Simulink using Simscape Electrical to model the electromechanical behavior of the SWIFT-UAV propulsion subsystem. The digital twin consists of three primary components: the battery model, the motor–ESC model, and the telemetry synchronization. Together, these subsystems form a high-fidelity virtual representation of the propulsion chain capable of synchronizing with physical telemetry and forecasting system behavior under dynamic load conditions.

The battery subsystem represents a 6-cell lithium-polymer (LiPo) pack configured in series, yielding a nominal pack voltage of 25.2 V. The pack has a rated capacity of 6 Ah. Each cell is modeled with state-of-charge (SOC) dependent open-circuit voltage characteristics and temperature-dependent internal resistance to capture nonlinear electrochemical behavior under varying operating conditions. Internal resistance was modeled as a function of both state of charge (SOC) and temperature to accurately reproduce load-induced voltage sag behavior. Resistance profiles were implemented using experimentally derived values at discrete SOC levels of 0, 0.1, 0.25, 0.5, 0.75, 0.9, and 1.0. Under a 5C discharge condition at 20°C, cell resistance varies from approximately 0.0117 Ω at 0% SOC to 0.0107 Ω at mid-range SOC. Temperature variation between 20°C and 40°C produces measurable resistance changes, which are incorporated into the model to account for thermal sensitivity during high-load operation.

The SOC state is updated through current integration, allowing the digital twin to track charge depletion dynamically during throttle transitions and sustained power demands. Similar digital twin frameworks for lithium-ion battery SOC and SOH estimation have been demonstrated in recent literature [10]. By incorporating SOC-dependent voltage curves and temperature-dependent resistance values, the battery model captures both steady-state and transient voltage response characteristics.

The motor–ESC subsystem captures the electromechanical coupling between throttle command, inverter switching behavior, and motor rotational dynamics. The motor is modeled as a three-phase, Y-connected brushless DC (BLDC) machine with eleven pole pairs (22 poles total). The rotor inertia is specified as 0.0005 kg·m^2, and the maximum flux linkage is defined as 0.0139 Wb. Due to the three-phase AC operation of BLDC systems, the motor is implemented using three-phase power electronics blocks within Simscape. The ESC is modeled as a three-phase, two-level inverter driven by pulse-width modulation (PWM) signals derived from throttle input. The ESC control chain consists of: throttle input normalized between 0 and 1, duty cycle mapping between 0.53 and 1, PWM generation at a switching frequency of 1 kHz, six-step commutation logic synchronized to rotor position feedback, and a gate drive signal applied to a three-phase inverter.

The inverter model incorporates non-ideal switching characteristics to improve electrical realism, including an on-state resistance of 0.001 Ω, a forward voltage drop of 0.8 V, and an off-conductance of 1×10^{-5} S. Switching devices are implemented using averaged switch blocks to maintain computational efficiency while preserving electrical fidelity within the propulsion subsystem model. Motor commutation is synchronized with rotor position via three virtual Hall sensors derived from the rotor's mechanical position. At each 60-degree electrical sector transition, the commutation pattern updates to maintain alignment between the stator flux and the rotor permanent magnet. This approach reproduces realistic torque production and current draw under varying throttle conditions.

The telemetry synchronization layer links measured signals from the physical propulsion system to the digital twin in real time. Voltage, current, throttle command, and rotational speed measurements are used to update and validate the virtual model. Two validation scenarios are supported. In the first scenario, identical throttle command sequences are applied to both the physical propulsion system and the digital twin model. Measured telemetry from the iron-bird configuration is logged and directly compared against simulation outputs. This approach evaluates model fidelity under matched control inputs and isolates modeling error. In the second scenario, the digital twin is initialized using measured battery state variables such as terminal voltage, SOC, and temperature. After initialization, model predictions evolve independently based on throttle inputs. This configuration evaluates forward-looking predictive capability and decouples model performance from real-time measurement noise, making it suitable for mission planning applications.

Through continuous synchronization with telemetry, the digital twin provides real-time and predictive estimates, transitioning the propulsion subsystem from passive monitoring toward predictive, model-informed energy management capable of supporting adaptive mission decision-making.

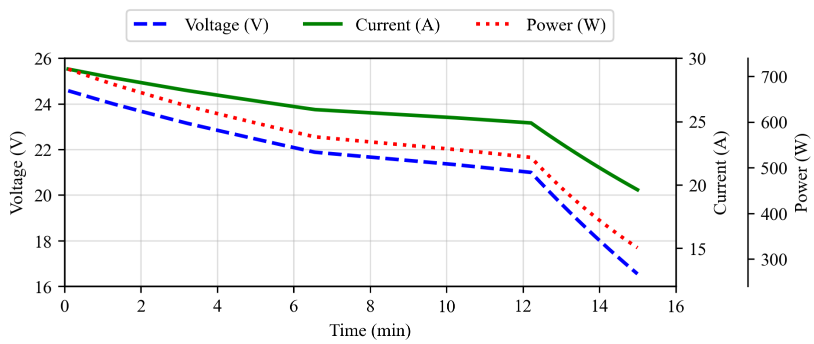

Fig. 3 Digital model battery voltage, current, and power response during 100% throttle propulsion testing.

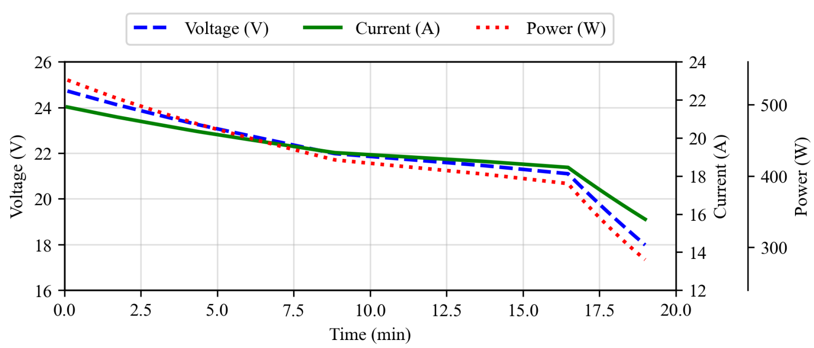

Fig. 4 Digital model battery voltage, current, and power response during 80% throttle propulsion testing .

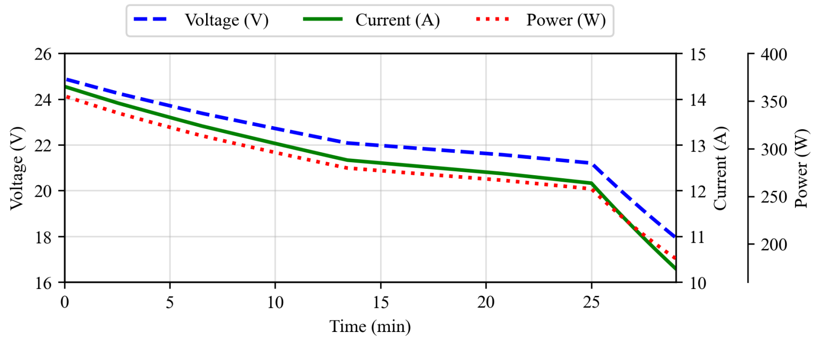

Fig. 5 Digital model battery voltage, current, and power response during 50% throttle propulsion testing .

B. Iron-Bird Propulsion Subsystem Configuration

The iron-bird propulsion test configuration replicates the SWIFT-UAV electrical propulsion chain while isolating it from aerodynamic and flight-control influences. The propulsion subsystem consists of a 6S LiPo battery pack, a 120 A-rated electronic speed controller (ESC), a three-phase brushless DC motor, pulse-width modulation (PWM) throttle control, and a 21-inch carbon fiber propeller. The battery pack has a nominal capacity of 6000 mAh and a discharge rating of 100C.

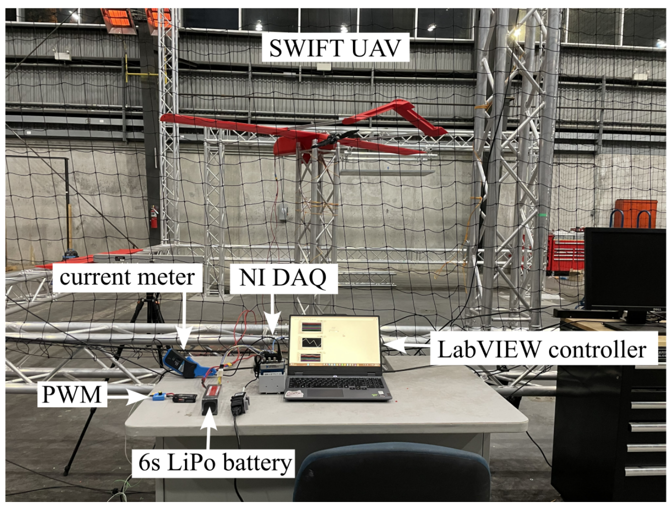

Fig. 6 Experimental set-up in UAV Cage.

Figure 6 shows that the airframe was rigidly secured to an aluminum extrusion mounting structure to prevent translation and rotational motion during operation, enabling controlled ground-based testing while the propulsion system was operated at various throttle settings. This configuration allows repeatable electrical load testing without the uncertainties introduced by aerodynamic lift, drag, and flight dynamics.

Battery voltage measurements were acquired using a National Instruments (NI) 9221 data acquisition module, with sensing leads connected across the battery pack terminals. Individual cell-level voltages were monitored to detect imbalance. Current measurements were obtained using an AC/DC Current Clamp (Model CC-65), interfaced with an NI 9215 module. Both modules were installed within an NI cDAQ-9174 chassis and controlled through a LabVIEW-based data acquisition system.

Voltage and current were sampled at a rate of 1 Hz, and electrical power was computed in real time as:

$$P(t) = V(t) \cdot I(t)$$

The selected sampling frequency was determined to be sufficient for capturing steady-state propulsion behavior during constant throttle testing. Moreover, each throttle condition was repeated only once.

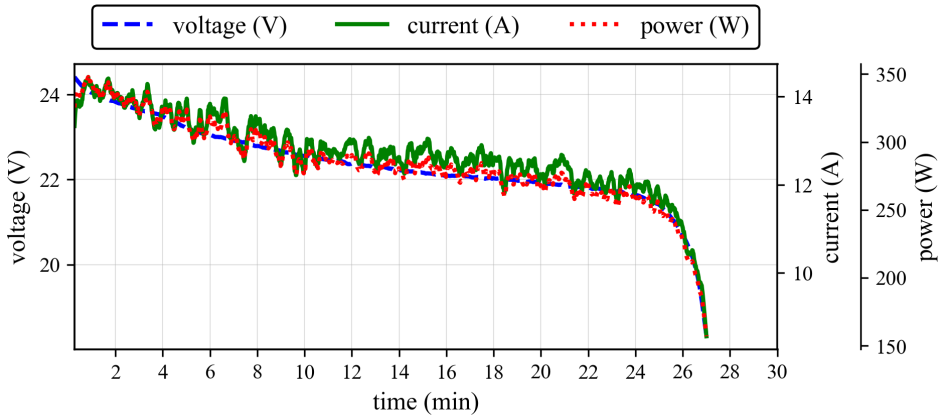

Fig. 7 Measured battery voltage, current, and power response during 50% throttle propulsion testing.

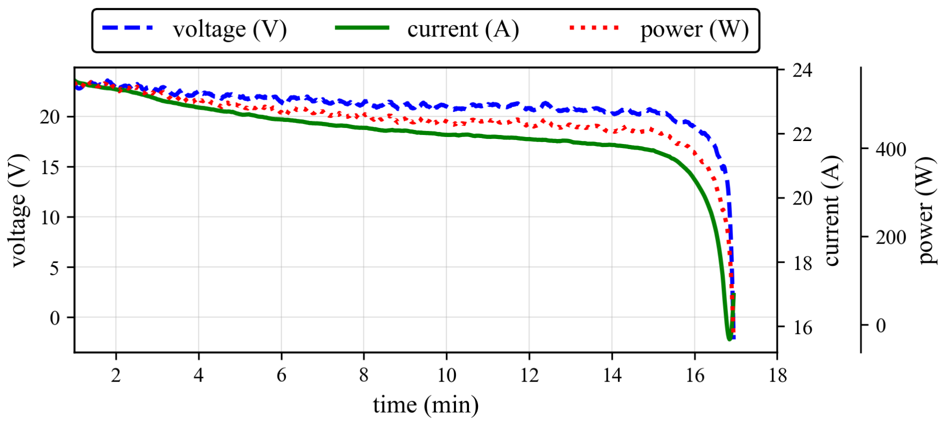

Fig. 8 Measured battery voltage, current, and power response during 80% throttle propulsion testing.

IV. Results

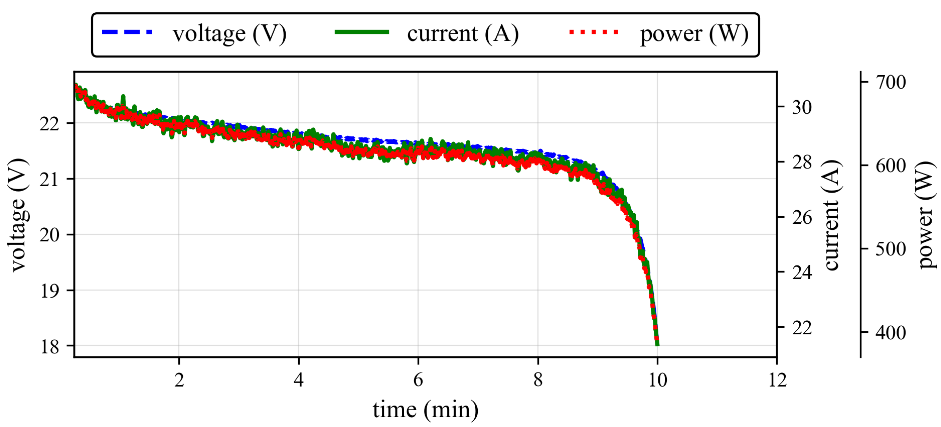

Fig. 9 Measured battery voltage, current, and power response during 100% throttle propulsion testing.

The propulsion subsystem was evaluated under sustained 50%, 80%, and 100% throttle conditions to assess digital twin performance across progressively increasing load regimes. For each case, state of charge (SOC), average C-rate, and projected steady-state endurance were computed from experimentally measured current and voltage data.

At 50% throttle, the average discharge rate was 1.79C, corresponding to approximately 10.7 A for a 6 Ah battery pack. The final state of charge (SOC) at the conclusion of the test was 19.4%, indicating substantial capacity utilization during the experimental duration. Based on the measured discharge rate, the digital twin projected an initial steady-state endurance of approximately 33.5 minutes under sustained 50% throttle conditions.

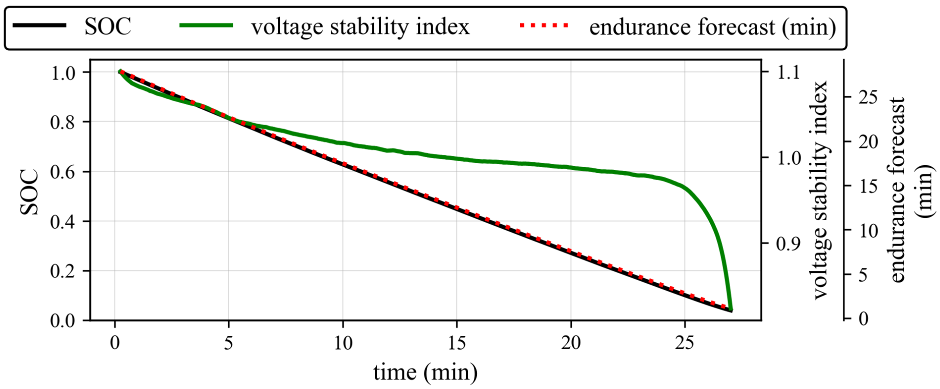

Fig. 10 Time evolution of state-of-charge (SOC), voltage stability index (VSI), and predicted remaining endurance under sustained 50% throttle loading.

At 80% throttle, the average discharge rate increased to 2.95C (approximately 17.7 A), and the projected endurance decreased to 20.4 minutes. The final SOC was 17.2%, reflecting increased energy consumption under elevated propulsion loading. The reduction in projected endurance relative to the 50% case is consistent with the higher current demand and associated resistive and electromechanical losses within the propulsion subsystem.

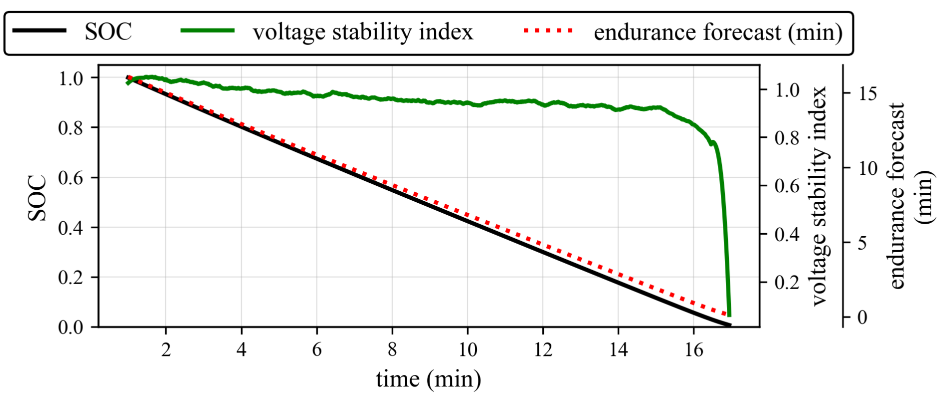

Fig. 11 Time evolution of state-of-charge (SOC), voltage stability index (VSI), and predicted remaining endurance under sustained 80% throttle loading.

At 100% throttle, the average discharge rate further increased to 3.99C, corresponding to approximately 23.9 A, producing a projected steady-state endurance of 15.1 minutes. The final SOC was 33.0%, again indicating limited total capacity depletion due to the short experimental duration, but under the highest instantaneous propulsion loading of the three cases.

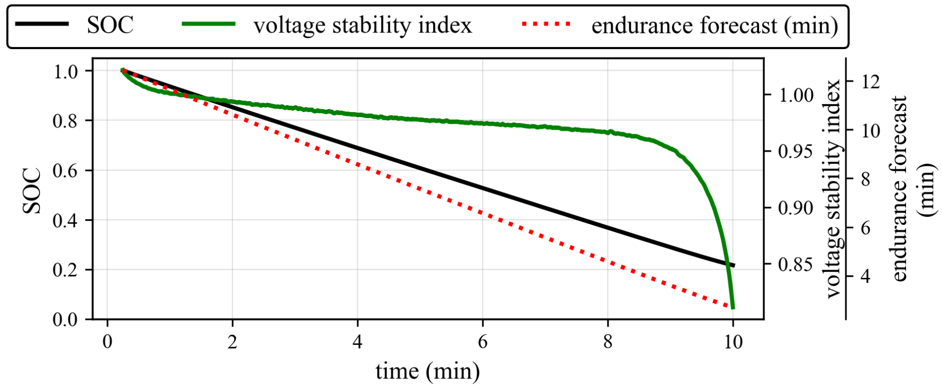

Fig. 12 Time evolution of state-of-charge (SOC), voltage stability index (VSI), and predicted remaining endurance under sustained 100% throttle loading.

Across all throttle levels, projected endurance decreased consistently with increasing C-rate. The reduction in estimated remaining useful life (RUL) follows the expected inverse relationship between discharge rate and endurance, indicating physically consistent model behavior. This trend validates the digital twin's ability to translate measured current demand into forward-looking mission endurance predictions while maintaining stable and responsive SOC estimation under elevated propulsion loading. The progressive increase in C-rate from 1.79C to 3.99C confirms that the model responds appropriately to changes in throttle command and associated current draw. Unlike earlier low-load validation cases, these tests operated within moderate-to-high discharge regimes, providing stronger validation of endurance forecasting under meaningful propulsion stress. The observed SOC evolution in each case demonstrates that the experiments primarily validate current tracking, voltage response, and endurance prediction logic rather than nonlinear low-SOC behavior or long-term degradation effects.

Table 1 Propulsion Subsystem Performance Summary at Varying Throttle Levels

Throttle (%)	Avg. Current (A)	Energy (Wh)	Endurance Forecast (min)
50	12.701	127.000	33.5
80	22.019	123.762	20.4
100	28.423	99.993	15.1

It should be noted that the propulsion motor used in this study is typically operated with a higher-voltage battery configuration, commonly 10S or 12S lithium-polymer packs, to achieve its full rated performance. However, due to laboratory availability constraints, a 6S LiPo battery was utilized for the present iron-bird validation experiments. Operating at a reduced supply voltage limited the achievable motor speed and overall power draw, resulting in comparatively moderate discharge rates even at 100% throttle. Consequently, the observed C-rates reflect subsystem-level validation under constrained voltage conditions rather than full operational flight loading. Future experiments employing higher-voltage battery configurations and extended-duration testing will enable validation under more representative propulsion stress conditions and deeper discharge regimes.

V. Conclusion

This work presented the ongoing development and subsystem-level validation of a propulsion digital twin for the SWIFT-UAV platform using a controlled iron-bird configuration. Experimental results demonstrate consistent SOC tracking and physically reasonable endurance forecasting trends across multiple throttle conditions. While the digital twin framework shows promising predictive capability, full real-time integration and in-flight validation remain under development. The insights gained from this study provide a foundation for continued refinement, hardware-in-the-loop implementation, and future flight testing.

VI. Acknowledgments

This work is supported by the National Science Foundation (NSF) under grant numbers ITE-2344357, CMMI-2152896, and CPS2237696. Additional funding for this work comes from the Office of Naval Research through award number 14048906. Any opinions, findings, conclusions, or recommendations expressed in this material are those of the authors and do not necessarily reflect the views of the National Science Foundation or the United States Navy. Additionally, this work was only possible with the help of Mumin Adhami and Thienan Hoang.

References

[1] Telli, K., Kraa, O., Himeur, Y., Ouamane, A., Boumehraz, M., Atalla, S., and Mansoor, W., "A Comprehensive Review of Recent Research Trends on Unmanned Aerial Vehicles (UAVs)," *Systems*, Vol. 11, No. 8, 2023, p. 400. doi:10.3390/systems11080400.

[2] Kaya, M. N., and Ural Bayrak, Z., "Detailed Analysis of Li-ion Batteries for Use in Unmanned Aerial Vehicles," *Turkish Journal of Science and Technology*, Vol. 19, No. 1, 2024, pp. 295–304. doi:10.55525/tjst.1437348.

[3] Boukoberine, M. N., Zhou, Z., and Benbouzid, M., "A critical review on unmanned aerial vehicles power supply and energy management: Solutions, strategies, and prospects," *Applied Energy*, Vol. 255, 2019, p. 113823. doi:10.1016/j.apenergy.2019.113823.

[4] Willcox, K., Bingham, D., Chung, C., Chung, J., Cruz-Neira, C., Grant, C., Kinter, J., Leung, R., Moin, P., Ohno-Machado, L., et al., *Foundational research gaps and future directions for digital twins*, National Academies Press Washington, DC, USA, 2023.

[5] Glaessgen, E., and Stargel, D., "The Digital Twin Paradigm for Future NASA and U.S. Air Force Vehicles," *Structural Dynamics and Materials Conference; 20th AIAA/ASME/AHS Adaptive Structures Conference*, American Institute of Aeronautics and Astronautics, 2012. doi:10.2514/6.2012-1818.

[6] Tuegel, E. J., Ingraffea, A. R., Eason, T. G., and Spottswood, S. M., "Reengineering Aircraft Structural Life Prediction Using a Digital Twin," *International Journal of Aerospace Engineering*, Vol. 2011, 2011, pp. 1–14. doi:10.1155/2011/154798.

[7] Xiong, R., Zhang, Y., Wang, J., He, H., Peng, S., and Pecht, M., "Lithium-Ion Battery Health Prognosis Based on a Real Battery Management System Used in Electric Vehicles," *IEEE Transactions on Vehicular Technology*, Vol. 68, No. 5, 2019, pp. 4110–4121. doi:10.1109/tvt.2018.2864688.

[8] Burnett, M., Garcia-Sandoval, M., Siuhi, D., Anandkumar, A., Morris, S., and Downey, A. R. J., "SWIFT UAV: Scientific Workhorse for In-Flight Testing," *ASME International Mechanical Engineering Congress and Exposition (IMECE 2025)*, American Society of Mechanical Engineers, 2025. NSF Research Poster Competition; Track 19-01; Poster ID IMECE2025-173844.

[9] Grieves, M., and Vickers, J., *Digital Twin: Mitigating Unpredictable, Undesirable Emergent Behavior in Complex Systems*, Springer International Publishing, 2016, pp. 85–113. doi:10.1007/978-3-319-38756-7_4.

[10] N, N., and Patange, S. S., "Digital-Twin Based SOC and SOH Estimation for Lithium-Ion Batteries," *International Journal of Scientific Research in Computer Science, Engineering and Information Technology*, Vol. 11, No. 6, 2025, pp. 240–247. doi:10.32628/cseit25116042.